JOURNAL OF GEOPHYSICAL RESEARCH, VOL. 105, NO. C12, PAGES 28,547–28,557, DECEMBER 15, 2000

Flow structure in depth-limited, vegetated flow

H. M. Nepf and E. R. Vivoni

Parsons Laboratory, Department of Civil and Environmental Engineering, Massachusetts Institute of Technology Cambridge, Massachusetts

Abstract. Aquatic vegetation controls the mean and turbulent flow structure in channels and coastal regions and thus impacts the fate and transport of sediment and contaminants. Experiments in an open-channel flume with model vegetation were used to better understand how vegetation impacts flow. In particular, this study describes the transition between submerged and emergent regimes based on three aspects of canopy flow: mean momentum, turbulence, and exchange dynamics. The observations suggest that flow within an aquatic canopy may be divided into two regions. In the upper canopy, called the "vertical exchange zone", vertical turbulent exchange with the overlying water is dynamically significant to the momentum balance and turbulence; and turbulence produced by mean shear at the top of the canopy is important. The lower canopy is called the "longitudinal exchange zone" because it communicates with surrounding water predominantly through longitudinal advection. In this region turbulence is generated locally by the canopy elements, and the momentum budget is a simple balance of vegetative drag and pressure gradient. In emergent canopies, only a longitudinal exchange zone is present. When the canopy becomes submerged, a vertical exchange zone appears at the top of the canopy and deepens into the canopy as the depth of submergence increases.

1. Introduction

Aquatic vegetation controls the mean and turbulent flow structure in channels and coastal regions and thus impacts the fate and transport of sediment and contaminants. The additional drag contributed by the plants reduces the mean flow within the canopy. The baffling of flow reduces the sediment load potential, and it promotes accumulation of sediment by reducing near-bed stress [*Lopéz* and *García*, 1998]. Vegetative drag can impact flood routing by significantly altering floodplain conveyance. It also influences wetland circulation and thus function [*Kadlec* , 1990, 1995]. Finally, new regions of turbulence production are created in the shear layer at the top of a canopy and in the wakes of individual canopy elements. The latter is particularly important for the emergent condition, for which shear generation is minimal. Although wake turbulence may augment the overall turbulence intensity, its small length scale reduces turbulent diffusivity relative to unvegetated conditions [*Nepf*, 1999].

A great deal is known about unconfined canopy flow through work on terrestrial canopies (Figure 1a), which is reviewed by *Raupach et al.* [1996]. A key feature is the development of a strong shear layer at the top of the canopy with a flow structure similar to a free shear layer. Turbulence produced within this layer defines the scale of active turbulence within and just above the canopy. Typically, the shear length scale, L_s, is of the order of the canopy height, h. Turbulence production within the wakes of canopy elements is secondary, contributing only 10% of the in-canopy turbulence [*Raupach and Shaw*, 1982]. The flow in the canopy is driven by turbulent stress, that is the vertical turbulent transport of momentum from the overlying flow, with negligible contribution from pressure gradients [*Raupach et al.* 1991].

The terrestrial canopy model may also be used to describe flow through deeply submerged aquatic canopies, that is for which the water depth, H, is large compared to the canopy height, h. For many aquatic canopies, however, the depth ratio, H/h, is not large (Figures 1b and 1c), and the limited depth may affect both the mean and turbulent flow. Several studies have experimentally or numerically examined the flow through submerged, aquatic canopies of flexible and rigid plant mimics [e.g., *Kouwen and Unny*, 1973; *Murato et al.*, 1984; *Lopéz and García*, 1996]. Only a few studies have examined the limiting condition of emergent vegetation (Figure 1c) [*Burke and Stolzenbach*, 1983; *Nepf*, 1999]. This paper explores the transition from the emergent (H/h =1) to the submerged regimes, considering momentum sources, turbulence, and exchange dynamics. Based on what is known about the deeply submerged and emergent canopy limits, the following trends are expected as the depth ratio, H/h, increases from 1. First, the flow forcing within the canopy shifts from predominantly pressure-driven to stress-driven. Second, the primary source of turbulence production shifts from stem wakes to the shear layer at the top of the canopy. Third, the principal mechanism for exchange with the surrounding water column shifts from longitudinal advection to vertical turbulent exchange. Observations presented in this paper better define these trends.

Finally, aquatic plants tend to have greater flexibility than their terrestrial counterparts, leading to a greater range of plant motion. With increasing flow speed, aquatic plants exhibit four regimes of motion: (1) erect, (2) gently swaying, (3) strong, coherent swaying (monami), and (4) prone [*e.g.*, *Murato et al.*, 1984, *Ackerman and Okubo*, 1993, *Grizzle et* al., 1996]. In this study we consider only

Paper number 2000JC900145.
0148-0227/00/2000JC900145$09.00

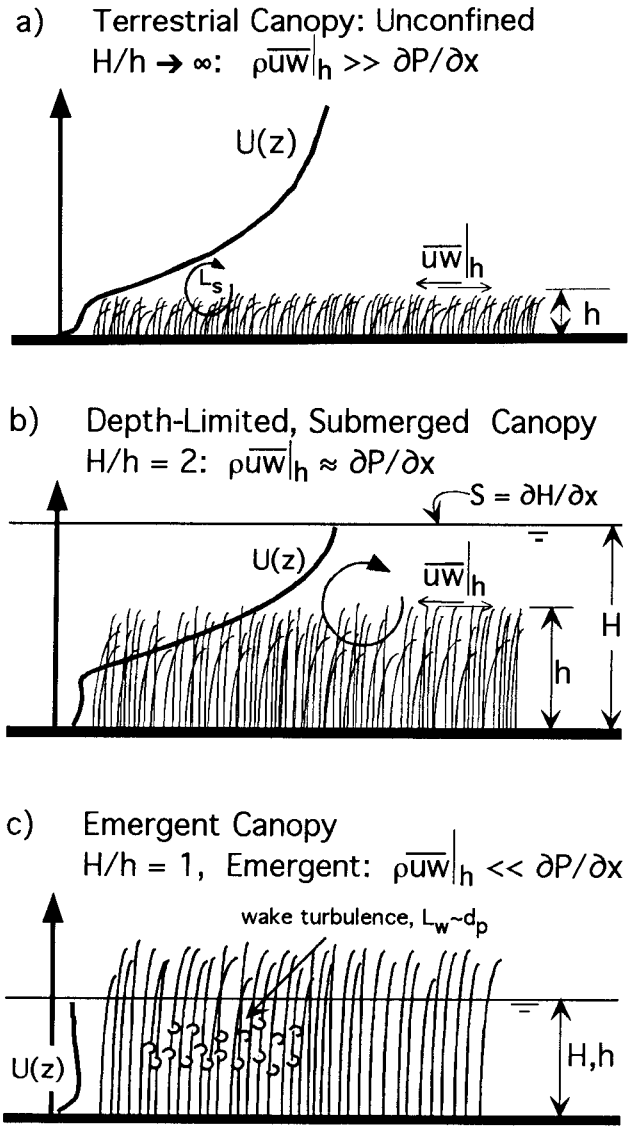

Figure 1. Velocity profiles, *U(z)*, for three depth ratios, *H/h*, where *H* is water depth and *h* is canopy height. (a) Terrestrial canopies represent the unconfined limit, *H/h* ' ∞, for which vertical turbulent transport of momentum from overlying flow controls flow within the canopy. (b) As the depth ratio decreases, pressure gradients, *∂P/∂x*, within the canopy become comparable to turbulent stress, . (c) As the depth ratio declines toward the emergent limit, *H/h* = 1, the turbulence scale shifts from predominantly shear generated, L_S, to predominantly wake generated, L_W, signaling a reduction in eddy scale.

the first two regimes, which have hydraulically similar behavior [Kouwen and Unny, 1973]. The stronger responses, monami and pronation, have significant additional impact on flow structure and are considered in an upcoming manuscript.

2. Experimental Methods

Laboratory experiments were conducted in a 24-m long by 38-cm wide, recirculating glass wall flume (Figure 2). The model canopy was 7.4 m long with a height h =16 cm. The model was constructed based on similarity in geometry and flexural rigidity to prototype aquatic vegetation, as reported by *Kouwen and Li* [1980]. Each plant consisted of six blades of width w = 0.3 cm, bundled to a short (2 cm), basal stem (diameter, 0.64 cm). The blades were made from a 0.025-cm-thick vinyl plastic. The morphology of a single plant is shown in Figure 3. The stems were mounted on a Plexiglas baseboard and distributed randomly based upon a computer-generated template. The rigidity of each branch is represented by the modulus of elasticity, E, and the moment of inertia, I, which together form the flexural rigidity, J. For the model $J = 1.0 \times 10^{-5}$ N m^2. For real grasses of comparable length (h = 10-20 cm), $J = 5 \times 10^{-6}$ to 1×10^{-3} *N m^2 [Kouwen and Li* 1980]. A similarity condition for J is the ratio of bending resistance to drag, F,

$$F = \frac{\text{drag}}{\text{rigidity}} = \frac{\rho U_h^2 h^3 w}{J},$$

with U_h the velocity at the top of the canopy and ρ the water density. For the model, F = 1 – 8. Estimates of F for field conditions were made for the same stem geometry (h, w) using J reported above and characteristic channel speeds of 0.1 to 1 m/s [*Kouwen and Li*, 1980]. F = 0.1 to 2000, with smaller values associated with erect plant posture, as considered here, and larger values associated with prone posture.

A steady, recirculating current was generated by a centrifugal pump and controlled by a diaphragm valve. The outlet was located in the bottom of the flume, 8 m downstream of the end of the canopy. An inlet pipe released water to the center of the flume 5 m upstream of the canopy's leading edge. Mats of rubberized fiber were used to dampen inlet turbulence, and a 0.5-m section of honeycomb was used to eliminate swirl. The canopy baseboard extended 3 m upstream of the canopy's edge and was tapered to the flume bottom. The flow depth was varied to produce depth ratios, *H/h* = 1.0, 1.25, 1.50, 1.75, 1.90, 2.15, 2.75, with

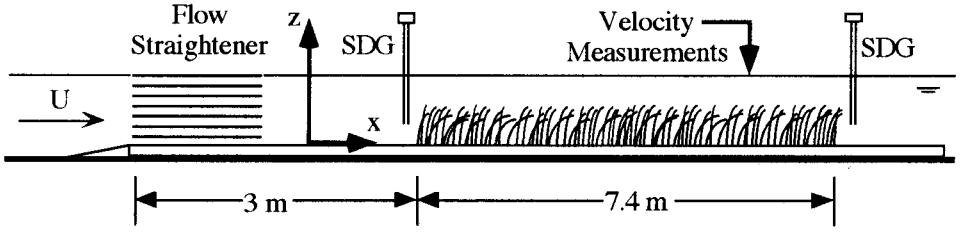

Figure 2. Experiments were conducted with a 7.4 m long model canopy fitted into a 24-m re-circulating flume. Velocity was measured using both acoustic Doppler (ADV) and laser Doppler (LDV) techniques. Surface slope was measured using two 0.2-mm resolution surface displacement gages (SDG). The streamwise coordinate is denoted by x, with x positive in the downstream direction, and the vertical coordinate is denoted by z, with z = 0 at the bed.

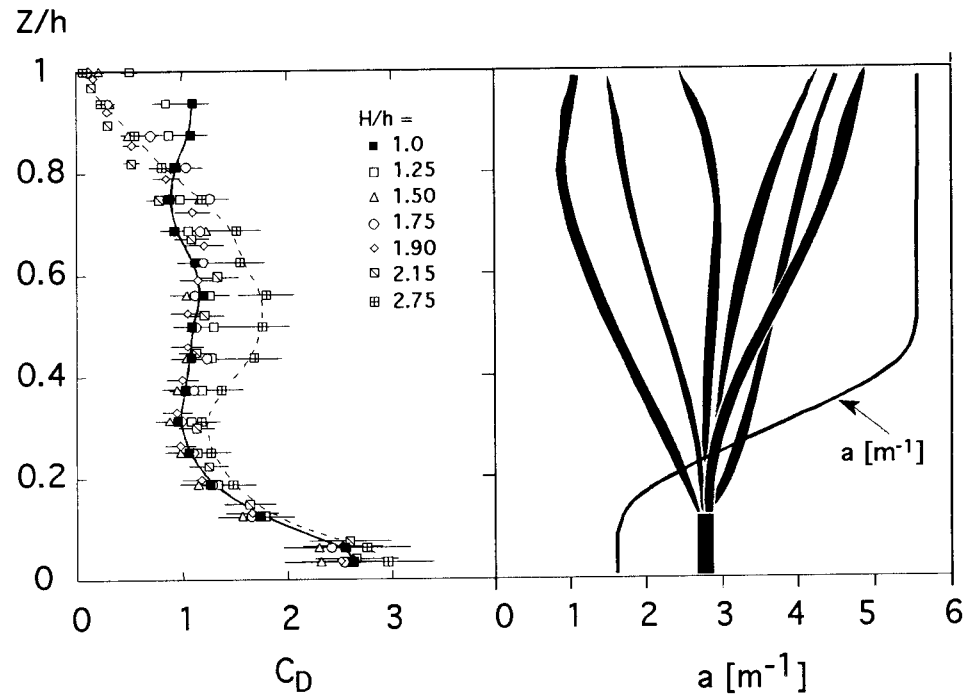

Figure 3. Profiles of vegetative drag, a (m^{-1}), solid line, and drag coefficient, $C_D(z)$, for several depth ratios, as indicated in figure. Horizontal bars represent uncertainty.

corresponding Reynolds number (UH/ν) between 4 x 10^3 and 4 x 10^4. These depth ratios focus specifically on the transition from emergent to submerged canopies, but also reasonably represent conditions in shallow coastal waters [*Orth and Moore*, 1988]. Vegetated zones have been recorded as deep as 90 m [e.g., *Duarte*, 1991]. These deeply submerged canopies (i.e. H/h >10) behave as unconfined canopies, described above and in previous literature [e.g., *Raupach et al.*, 1996].

The model meadow extended from wall to wall to prevent elevated flow close to the wall. A single stem density, n = 330 plants m^{-2}, was considered. The blockage provided by the canopy is characterized by its frontal area per volume, called the canopy density, a [e.g., *Kaimal and Finnigan*, 1994]. The frontal area, A_f of ten randomly selected plants was estimated at centimeter intervals in the vertical, Δz = 1 cm, by tracing the plants' silhouettes onto grid paper. Averaging over the ten plants, the canopy density was then calculated as

$$a(z) = nA_f(z)/\Delta z \quad (1)$$

The profile of $a(z)$ is shown in Figure 3.

Mean (U, V, W) and turbulent (u, v, w) velocities corresponding to the stream-wise (x), lateral (y), and vertical (z) directions, respectively, were measured using three-dimensional acoustic Doppler velocimetry (ADV) and 2-D laser Doppler velocimetry (LDV) at a test section located 6.6 m from the leading edge. Longitudinal transects through the array demonstrated that this position was representative of uniform flow conditions, that is, not affected by the leading edge. The canopy extended 80 cm beyond this point, such that the sampling region was fully within the canopy model. The ADV could be deployed without disturbance to the array configuration; that is, interference by canopy elements entering the sampling volume was not a problem. However, the LDV typically required the displacement of two to three plants to clear its optical path. Six-minute records were collected at 25 and 50 Hz for the ADV and LDV, respectively. The velocity uncertainty was 0.1 cm/s for the ADV and 0.2 mm/s for the LDV. Because the flow field within the canopy was inhomogeneous at the stem scale, a horizontal average of three lateral positions, denoted by angle brackets, was used to represent the mean, homogeneous (in x and y) velocity statistics [e.g., *Kaimal and Finnigan*, 1994, p. 84]. Temporal averages are denoted by an overbar. The sidewall boundary layers, defined by a significant contribution of sidewall shear, were less than 5 cm owing to the dominance of vegetative drag. A region of 30 cm at the center of the flume was reasonably free from wall effects. The lateral positions were chosen to lie inside this region, and to avoid locations directly behind individual stems. Finally, differential roughness between the glass walls and the top of the canopy can set up a secondary circulation above the canopy, moving from the centerline toward the walls just above the canopy. A detailed lateral transect just above a model canopy showed this secondary flow to be less than 3 mm/s [*Ghisalberti*, 2000].

The surface slope, $\partial H/\partial x$, was measured using a pair of resistance-type surface displacement gages (SDG in Figure 2) with 0.2-mm resolution, positioned 5 cm upstream and downstream of the canopy. The reference for zero surface slope was recorded with the pump turned off (zero flow). After the pump was turned on, several minutes were required before transient long waves dissipated and a steady flow condition was achieved. The uncertainty of the slope measurement was 3 x10^{-5}, or roughly 10%, arising predominantly from the resolution of the gages.

The canopy drag coefficient, $C_D(z)$, was estimated from

the surface slope and from profiles of Reynolds stress, $<\overline{uw}>$, using the horizontally averaged momentum equation [e.g., *Dunn et al.* 1996], that is,

$$0 = -g\frac{\partial H}{\partial x} - \frac{\partial <\overline{uw}>}{\partial z} - \frac{1}{2}C_D a <U>^2. \qquad (2)$$

Note that (2) neglects a correction to the body force, $g\partial H/\partial x$, for water volume excluded by plant volume. For this model the correction is negligible (< 1%), but may contribute to the dependence $C_D(a)$ at high canopy density [*Dunn et al.*, 1996]. In addition, viscous stress, $\nu\partial u/\partial z$, and bed drag are excluded because they are negligible compared to the vegetative drag. The profiles $C_D(z)$ are shown in Figure 3, and discussed below.

The velocity records were also used to explore the following terms in the turbulent kinetic energy budget: the total turbulent kinetic energy, $k = (\overline{u^2} + v^2 + w^2)/2$; the vertical turbulent transport, $T_t = \partial <\overline{wk}> /\partial z$; and the bed shear production, $P_s = -<\overline{uw}>(\partial <U>/\partial z)$. The turbulence production associated with canopy wakes, P_w, was estimated as the work input by the vegetative drag, that is, per unit mass [e.g., *Burke and Stolzenbach*, 1983],

$$P_w = \frac{1}{2} C_D a <U>^3. \qquad (3)$$

This assumes that all energy extracted from the mean flow by plant drag appears as turbulent kinetic energy, which depends on the plant-scale Reynolds number, $Re_p = d_p U/\nu$, where d_p is the stem diameter or blade width. When $Re_p < \approx$ 200, wakes are not fully turbulent, and viscous drag, which contributes to turbulence production only indirectly through the generation of wake shear, becomes increasingly important. Thus for $Re_p < \approx 200$, P_w is over-predicted by (3). Here, $Re_p = 80$ - 4500, such that the dependence of (3) on Re_p is an important consideration, as discussed in section 3.3.

Within terrestrial canopies the wake production is often estimated using the approximation, $P_w \approx U\partial <\overline{uw}>/\partial z$. This estimate assumes that the streamwise pressure gradient and bed slope are insignificant [*Raupach et al.*, 1991], such that the momentum equation (2) reduces to a balance of shear stress and vegetative drag. While this estimate may be a useful simplification for deeply submerged flows, it cannot be used when the surface and/or bed slope are dynamically important, as in this experiment.

Finally, the rate of turbulent dissipation, ε, was evaluated by comparing the spectra from the longitudinal and vertical velocity components to an inertial subrange fit,

$$S_{uu} = A\frac{18}{55}\varepsilon^{2/3}(U/(2\pi))^{2/3} f^{-5/3}; \quad S_{ww} = \frac{4}{3}S_{uu}, \qquad (4)$$

where $A \approx 1.5$ is an experimentally determined, universal constant for turbulent flows [e.g., *Kundu*, 1990, p. 441]. In regions of high turbulence intensity, this technique overestimates the true dissipation rate due to aliasing of energy between adjacent wave numbers [*Lumley*, 1965]. This limitation becomes important near the top of submerged canopies, where turbulence intensity is high, and is indicated in data presentation.

3. Results and Discussion

3.1. Drag Coefficient

The range of canopy drag coefficient, $C_D(z)$ observed here (0.1 – 3, Figure 3) is similar to values observed for terrestrial canopies (0.2 – 2) [*Brunet et al.*, 1994] and for other models of submerged vegetation (0.5-1.5)[*Dunn et al.*, 1996]. Over the lower half of the canopy ($z/h < 0.3$, Figure 3), $C_D(z)$ increases toward the bed, reflecting the increasing importance of viscous effects with decreasing Re_p. The stems near the bed are cylindrical, and the observed values, C_D = 1-3, agree with literature values at the observed Reynolds numbers, Re_p = 100-200 [e.g., *Munson et al.*, 1990]. This agreement suggests that neglecting bed drag relative to stem drag, as done to calculate C_D in (2), is appropriate even close to the bed. Note that this approximation may not extend to field conditions, where natural substrates are much rougher than the Plexiglas bed of the model. Above the bed the emergent canopy (solid squares in Figure 3) produces a constant value of $C_D \approx 1$. When the canopy is submerged, however, C_D diminishes toward the top of the canopy ($z/h > 0.8$) due to a relaxation of form drag as flow bleeds around the free end. A similar trend has been observed in terrestrial canopies [*Brunet et al.*, 1994]. Except at the top of the canopy, the profiles of C_D estimated under different depths of submergence agree. The exception is $H/h = 2.75$, for which $C_D(z)$ increases at mid-depth. The cause of this variation is unclear.

3.2. Mean Flow Structure

Profiles of mean velocity and Reynolds stress are shown in Figure 4 for the emergent (H/h =1) and maximally submerged ($H/h = 2.75$) cases under the same surface slope. In these figures the horizontal bars indicate the standard deviation between the three lateral positions. This variability greatly exceeds the uncertainty of individual measurements. Within the emergent canopy (Figure 4a) vertical turbulent transport of momentum is negligible, that is, $<\overline{uw}> \approx 0$, and the momentum equation, (2), reduces to a balance of pressure gradient and vegetative drag. Because the longitudinal pressure gradient is not a function of z, vertical variation in velocity (Figure 4a) reflects the variation in canopy density (Figure 3), increasing toward the bed as $a(z)$ decreases. The turbulent velocities (Figure 4b) mirror the mean velocity distribution, with the horizontal turbulent rms velocities 30% higher than the vertical turbulent rms velocity.

For the submerged condition, (Figure 4c) the drag discontinuity at the top of the canopy produces a strong shear layer. This leads to a significant contribution from Reynolds stress in the region of $z/h = 1$ that is not seen under the emergent condition. The Reynolds stress peaks just below the top of the canopy and decays downward into the canopy. Vertical penetration of turbulent stress into the canopy is a measure of the region within the canopy that actively exchanges momentum, and by inference other properties, with the overlying water. The extent of this region may be defined as the point within the canopy at which the turbulent stress has decayed to 10% of its maximum value. This position will be called the penetration depth, $z = h_p$.

The submerged canopy is divided into two zones, above and below the penetration depth. Using the context of exchange with surrounding water, the two regions are named the longitudinal exchange zone ($z < h_p$) and the vertical-exchange zone ($z > h_p$). Within the longitudinal exchange zone vertical turbulent transport of momentum is negligible, that is, $<\overline{uw}> \approx 0$, and the flow is determined by a balance

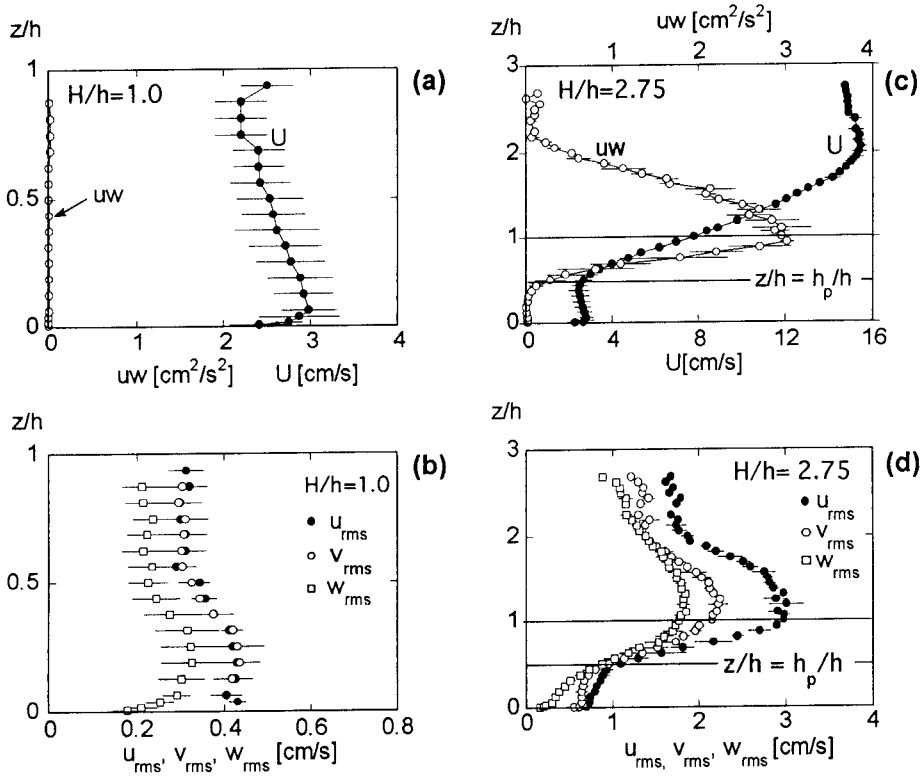

Figure 4. Mean velocity, turbulent stress, and turbulent rms observed for (a, and b) emergent (H/h =1.0) and (c, and d) submerged (H/h =2.75) canopies. Each measurement represents the average of three lateral positions. Horizontal bars indicate the variability between lateral positions.

of pressure gradient (and/or bed slope, which is zero here) and vegetative drag. These conditions are the same as those observed in an emergent canopy (Figure 4a), for which we take $h_p = h$. That is, the flow forcing within the lower part of the submerged canopy is identical to that in the emergent canopy. Consistent with this, comparable flow speeds are observed in both the emergent and submerged canopy at vertical positions below the penetration depth of the submerged canopy, that is, $z < h_p$ (Figures 4a and 4c). Within the longitudinal exchange zone, and throughout the emergent canopy, the transport of scalars is dominated by advection from the leading edge of the canopy, known as blow-through, with minimal vertical exchange with the overlying water column.

Within the vertical exchange zone, $z > h_p$, vertical turbulent exchange (turbulent stress) contributes to the momentum balance within the canopy, and by analogy contributes to scalar exchange as well. The pressure gradient and associated longitudinal transport are still present in the vertical exchange zone for the depths of submergence shown in Figure 4c, but become less important as the depth of submergence increases further. The role of submergence depth in determining the flow forcing is demonstrated as follows. Within the canopy the turbulent stress gradient can be approximated as

$$\frac{\partial < \overline{uw} >}{\partial z} = \frac{< \overline{uw} >|_h}{(h - h_p)} \sim \frac{< \overline{uw} >|_h}{h}. \qquad (5)$$

Note that the rightmost term in (5) under predicts the stress gradient unless turbulent stress penetrates to the bed ($h_p = 0$). From the momentum balance of the flow above the canopy,

$$< \overline{uw} >|_h = g \frac{\partial H}{\partial x}(H - h). \qquad (6)$$

Using (6) to replace $< uw >|_h$ in (5), the ratio of the pressure gradient to the turbulent stress gradient inside the canopy is

$$\frac{\text{turbulent stress}}{\text{pressure}} = \frac{\partial < \overline{uw} > / \partial z}{g\, \partial H / \partial x} \sim \frac{H}{h} - 1. \qquad (7)$$

A similar relation describes the contribution of bed slope, with $\partial z_b / \partial x$ replacing $\partial H / \partial x$, where z_b is the position of the bed. For emergent conditions (Figure 1c, H/h = 1), (7) indicates that turbulent stress makes no contribution to the momentum balance, consistent with Figure 4a. For $H/h \rightarrow \infty$ the pressure gradient becomes negligible, consistent with observations within terrestrial canopies [e.g., *Finnigan*, 1979]. The real ratio of momentum forcing was estimated for each depth ratio using the stress gradient observed in the upper canopy (see, e.g., Figure 4c) and the measured surface slope (Table 1). As the depth ratio increased, the real momentum ratio also increased (Table 1), consistent with the scaling given in (7). As expected for $h_p > 0$ (see above), the observed ratios exceed those predicted by (7).

The relative magnitude of the pressure-driven and turbulent-stress-driven flow within the canopy has important implications for scalar transport, because they represent different modes of exchange between the macrophyte system and the surrounding water, longitudinal and vertical exchange, respectively. For a common range of submergences, $H/h \approx 1$ to 5, (7) suggests that both forms of exchange will be important, such that two sources of material exchange should always be considered; exchange with the overlying water column and exchange with the

Table 1 . Canopy Parameters

Run	H/h ± 0.03	$\partial H/\partial x$ x10^{-4} ± 0.3	Stress Pressure ± 0.1 from (7)	L_s/h ± 0.03	d/h ±0.03	u^* $\sqrt{gS(H-d)}$ ± 0.2 cm/s	z_o/h ±0.01
1	1.0	2.0					
2	1.25	2.8	0.6	0.37	0.89	1.3	0.03
3	1.50	2.5	0.8	0.61	0.79	1.7	0.05
4	1.75	2.5	1.2	0.67	0.75	2.0	0.09
5	1.90	5.0	1.5	0.72	0.74	2.9	0.07
6	2.15	8.3	1.6	0.71	0.72	3.9	0.07
7	2.75	2.0	2.0	0.69	0.70	2.5	0.11

underlying blow-through layer. In the limit of unconfined canopies, (7) suggests that only vertical turbulent exchange is important. This is consistent with observations in terrestrial canopies, for which momentum (and scalar) transport is dominated by vertical turbulent exchange.

Finally, note that a local velocity maximum appears near the bed (z/h = 0.1) for both emergent and submerged conditions (Figure 4a and 4c). As described above, this reflects the decrease in vegetative density (drag) in the sheath region of the canopy (Figure 3). Similar velocity maxima have been observed in real aquatic systems of emergent marsh [*Leonard and Luther*, 1995] and submerged sea grasses [*Ackerman and Okubo*, 1993], and have also been attributed to vertical variation in plant morphology. Near-bed velocity maxima have been observed in terrestrial canopies, but cannot be attributed to vertical variation in vegetative density because pressure forcing is negligible. Instead, the secondary maxima within terrestrial canopies are attributed to counter-gradient fluxes of momentum arising from large-scale motions (sweep events) that transport momentum from above directly into the lower regions of the canopy [*Shaw*, 1977].

Several researchers have noted that the flow over the top of submerged vegetation follows a logarithmic profile [e.g., *Gambi et al.* 1990; *Shi et al.*, 1995]. We also observe a logarithmic structure above the canopy for the depths ratios greater than 1.25. The overflow profile,

$$< U > (z) = \frac{u^*}{k} \ln((z-d)/z_o), \qquad (8)$$

is defined by three parameters: the zero-plane displacement, d, the friction velocity, u^*, and the roughness height, z_o[e.g., *Thom*, 1971]. The zero-plane displacement corresponds to the mean level of momentum absorption,

$$d = \int_0^h \frac{d < \overline{uw} >}{dz} z\, dz \Big/ \int_0^h \frac{d < \overline{uw} >}{dz} dz, \qquad (9)$$

and is related to the penetration depth, h_p, as both are measures of the distance into the canopy that momentum penetrates. We expect $d \sim h_p$, so that d provides an estimate for h_p that only requires velocity measurements above the canopy. Further discussion is given in section 3.4.

For flow above the canopy, $z = d$ is an effective lower boundary and thus $(H-d)$ is the effective depth of the overflow. A friction velocity for the overflow may then be estimated as

$$u^* = (gS(H-d))^{1/2}, \qquad (10)$$

which parameterizes the equivalent bed stress provided by the canopy on the overlying flow and appearing to act at $z = d$. Finally, using (9) and (10), the roughness length, z_o, is estimated by fitting the observed data to (8). An example is shown in Figure 5. The parameters d, z_o and u_* are summarized for each run in Table 1. As H/h increases, d/h decreases, indicating that the mean level of momentum absorption is pushed downward into the canopy. As the effective lower boundary is pushed downward (d/h decreasing), the canopy protrudes further upward into the overflow, providing a greater effective bed roughness, that is, z_o/h increases.

Within the logarithmic region the eddy viscosity may be modeled with inertial sublayer scaling [e.g., *Nezu and Rodi*, 1986] using an effective lower boundary at $z = d$. For comparison, ν_t was estimated from observed profiles of Reynolds' stress and profiles of mean shear calculated by central difference,

$$\nu_t = \frac{< \overline{uw} >}{\partial < U > / \partial z}. \qquad (11)$$

Above the canopy the model matches well the estimated eddy viscosity (Figure 5b). However, inside the canopy the model under predicts ν_t because it assumes eddy-scales approach zero at the effective bed location ($z = d$), which is not the case in the real canopy.

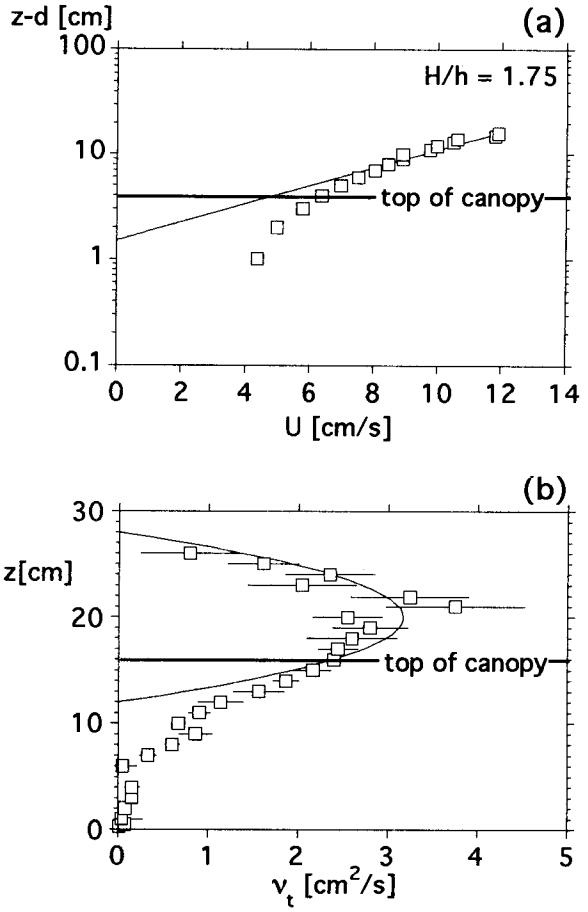

Figure 5. (a) Mean velocity profile and logarithmic profile fit for submerged canopy, H/h = 1.75. Friction velocity, $u_* = \sqrt{g\, \partial H/\partial x\, (H-d)}$, as in Table 1. (b) Eddy viscosity estimated from mean shear and turbulent stress profiles (squares) compared to inertial layer theory for an open channel flow beginning at d, the zero-displacement height, $d < h$.

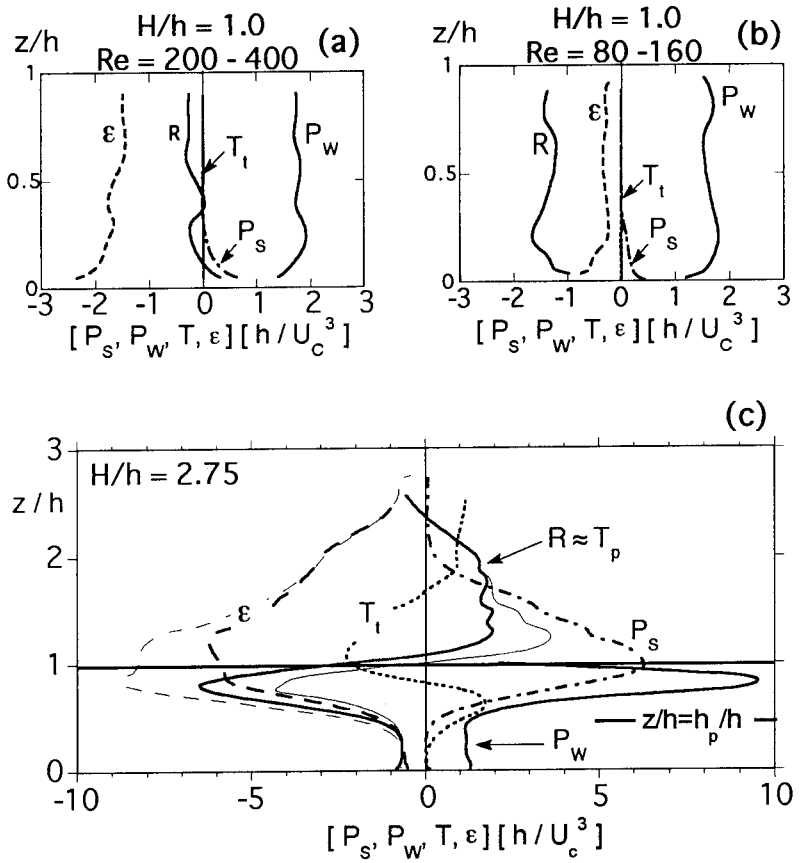

Figure 6. Turbulent kinetic energy for emergent and submerged conditions: (a) H/h = 1.0, Re_p = 200-400; (b) H/h = 1.0, Re_p = 80-160; (c) H/h = 2.75. Each term is normalized by the vegetation height, h, and the characteristic velocity, $U_c = (ghS)^{1/2}$, where S is surface slope. P_S is mean shear production. P_W is wake production. ε is dissipation rate. T_t is turbulent transport. R is the residual of the other terms.

3.3. Turbulent Energy Budget

Assuming steady, homogeneous flow and neglecting viscous stresses, the turbulent kinetic energy budget within a canopy may be expressed as [e.g., *Brunet et al.*, 1994]

$$\frac{D\langle \tilde{k} \rangle}{Dt} = 0 = P_s + P_w + T_t + T_p + \langle \varepsilon \rangle. \quad (12)$$

The shear production, P_s, wake production, P_w, dissipation, ε, and turbulent transport, T_t, are estimated from velocity measurements, as described above. The pressure transport, $T_p = \partial \langle wp \rangle / \partial z$, is difficult to measure directly and instead is estimated as the residual (R) of the remaining terms, as suggested by *Brunet et al.* [1994], that is,

$$T_p \approx R = -(P_s + P_w + T_t + \langle \varepsilon \rangle). \quad (13)$$

Note that we exclude dispersive transport and turbulence production by plant motion as these terms are negligible in rigid canopies or those of limited plant motion [*Kaimal and Finnigan*, 1994], as is considered here. The turbulent kinetic energy budget is shown in Figure 6 for two emergent canopies (Figures 6a and 6b) and one submerged canopy (Figure 6c). Each term is normalized by the canopy height, h, and a characteristic canopy velocity, $U_c = (gh\,\partial H/\partial x)^{1/2}$.

For emergent conditions (H/h =1), mean shear production, P_s, is small and occurs only near the bed. For natural substrates, additional turbulence may be generated by bed roughness. The turbulent transport, T_t, is negligible. This should leave a balance between estimated wake production, P_w, and dissipation, ε. This balance is observed when $Re_p >$ 200 (Figure 6a), for which wake production is correctly predicted by (3). When $Re_p < 200$, however, (3) overpredicts P_w, as shown in Figure 6b, for which Re_p = 80-160 and the estimated P_w does not balance ε. In this case the residual, R, is not an accurate predictor of pressure transport.

The submerged conditions are shown in Figure 6c for the depth ratio H/h = 2.75. Note that high turbulence intensity near the top of the canopy (Figure 4d) leads to an overprediction of dissipation rate in this region, as discussed earlier. Both the fitted dissipation rate (thin line) and the adjusted rate (based on *Lumley* [1965], thick line) are shown in Figure 6c. Similarly, two estimates are given for the residual (R). In the submerged case, shear generated at the top of the canopy provides an important source of turbulence, P_s, within the vertical exchange zone. Shear production is comparable to wake production, P_w, in this region. Additional turbulence generated above the canopy (P_S) is supplied to this region by turbulent transport, T_t. This additional source is partially balanced by the pressure transport, $T_p \approx R$, which has similar structure but is opposite in sign to T_t. Specifically, $T_p/T_t \approx$ -1.5-3. In a terrestrial canopy model, *Brunet et al.* [1994] found similar behavior with a ratio, $T_p/T_t \approx$ -0.8.

The longitudinal exchange zone, $z < h_p$, again resembles an emergent condition, as both T_t and P_S are negligible,

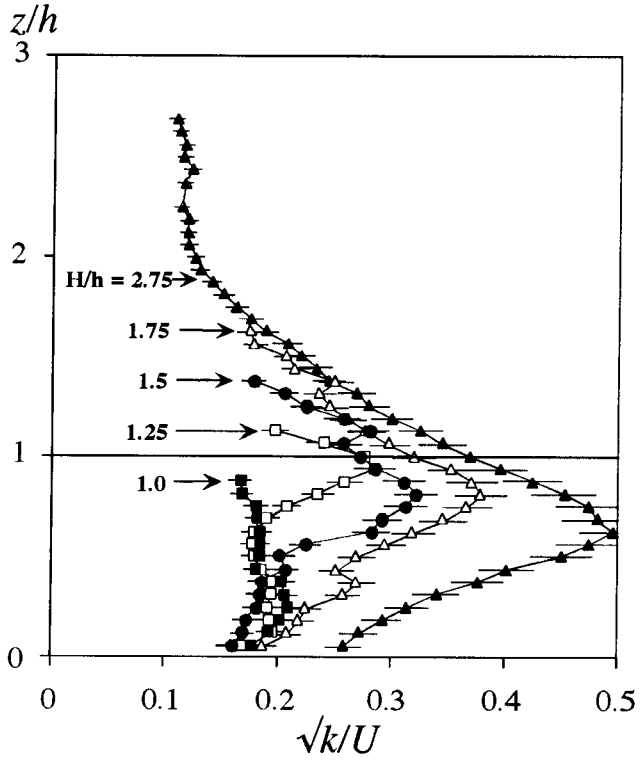

Figure 7. Normalized turbulent kinetic energy, $k(z)/U(z)$, for H/h = 1.0 (solid squares), 1.25 (open squares), 1.50 (solid circles), 1.75 (open triangles), 2.75 (solid triangles).

leaving $P_w \approx \varepsilon$. In this region $Re_P < 200$, such that P_W is overpredicted, which is reflected in the residual term. In contrast to this aquatic canopy the lower region of a terrestrial canopy exhibits the balance $T_t \approx \varepsilon$ [*Raupach et al.*, 1991]. This difference arises from the relative magnitudes of pressure and stress terms described by (7). In deeply submerged canopies blow-through (pressure-driven flow) is negligible such that near-bed velocity and associated P_W and P_S are small, and T_t is the main turbulence source. For shallow depth ratios, blow-through maintains U and P_w near the bed. When $P_W > T_t$, then $P_W \approx \varepsilon$, as seen here.

We can examine profiles of total turbulence intensity, $\sqrt{k}/U$, to further examine the relative contributions made by wake and mean shear production (Figure 7). For the emergent condition (solid squares, Figure 7), the turbulence intensity is fairly uniform over depth with $\sqrt{k}/U = 0.18$. As shear production is negligible in an emergent canopy (Figure 6), the observed turbulence entirely reflects wake generation. The emergent condition may also be used as a baseline for wake generation in the submerged canopies. This is justified because the contribution of wake production to $\sqrt{k}$ scales as $[adC_D]^{1/3}$ [e.g., *Raupach and Shaw*, 1982], which does not change appreciably with canopy submergence, except at the top of the canopy where C_D is diminished for submerged canopies (Figure 3). For the submerged canopies, $\sqrt{k}/U$ is enhanced (relative to the emergent profile) in the vertical exchange zone, consistent with the location of mean shear production, P_S, and contribution from vertical transport, T_t(Figure 6). The shear contribution increases in both magnitude and vertical extent as the depth ratio increases, reflecting a deeper penetration of P_S and T_t into the canopy. Although peak turbulent rms velocities occur at $z = h$ (Figure 4d), $\sqrt{k}/U$ peaks below this level. This structure is also observed in each individual component, for example, u_{rms}/U, and arises because U falls off more rapidly than $\sqrt{k}$ within the canopy. Measurements made with real sea grass in a flume also showed peaks in longitudinal intensity, u_{rms}/U, below the top of the canopy [*Gambi et al.*, 1990]. The peaks are less distinct, however, as the top of the real canopy was less well defined due to the natural variation in leaf length.

Using the emergent condition as a baseline for the wake contribution, the fraction of $\sqrt{k}/U$ attributed to wake generation can be estimated for each depth ratio (Figure 8). Note that the submerged canopy estimates are upper bounds, as the true wake production within a submerged canopy is expected to be a bit less than that observed in the emergent canopy due to the decrease in C_D toward the top of the submerged canopy (Figure 3). Figure 8 suggests a shift away from small-scale wake turbulence as the depth of submergence increases from 1 (emergent). For the deepest canopy considered, $H/h = 2.75$, wake turbulence contributes only 45%. Yet, for this canopy, $P_W \approx 2P_S$ (Figure 6). This disparity occurs because wake turbulence dissipates more rapidly than the larger scale shear turbulence, whose scale, L_S, is set by the mean shear [*Raupach et al.*, 1996],

$$L_S = \frac{\overline{U}\big|_h}{\left(\partial \overline{U}/\partial z\right)\big|_h}. \tag{14}$$

For the canopies considered here, $L_S = 0.37 - 0.72\ h$ (Table 1). The lowest value of L_S occurs for the smallest depth ratio H/h, suggesting L_S is limited by flow depth. This is discussed further in the following section. In contrast, wake turbulence, L_W, scales on the canopy elements, for example, the stem diameter, $d_P \approx 0.03h$, in this study. The disparity in scales in the model canopy, $L_S/L_W \approx 20$, explains the disproportionate contribution of shear production to observed turbulence levels. In terrestrial canopies the length scale disparity is much greater, $L_S/L_W \approx 1000$, and the

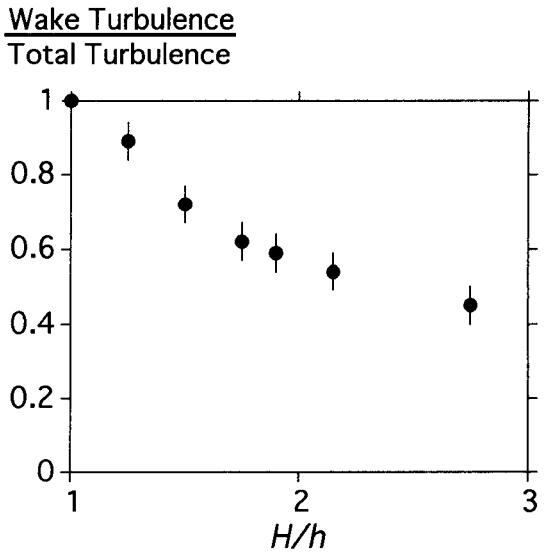

Figure 8. Fraction of turbulence attributed to wake generation. Emergent profile used as baseline for representative wake generation in submerged canopies.

contribution of wake turbulence is accordingly diminished, with only 10% of total turbulent kinetic energy in a forest canopy attributed to wake generation, despite the fact that $P_W \approx P_S$ within the canopy [*Raupach and Shaw*, 1982]. Because the length-scale ratio is generally smaller in aquatic systems, L_S/L_W= 20-100, we infer that wake turbulence will be generally more important in aquatic than in terrestrial systems, even for large depths of submergence. That is, even as the depth ratio increases, the contribution of wake turbulence may never decline to the terrestrial limit of 10%.

Finally, the correlation coefficient, $r = \overline{uw}/(u_{rms} w_{rms})$, is relatively large within the vertical exchange zone, r = -0.5, indicating that the turbulence in this region is very efficient in the vertical transport of momentum (and by analogy scalars); that is, the transport per unit of turbulence is high. This efficiency arises, in part, from the large scale of the shear layer turbulence, L_S. In contrast, within an emergent canopy or within the longitudinal exchange zone of a submerged canopy, wake turbulence dominates, and the turbulent scales are reduced to L_W. The small eddy scale makes turbulent transport within these regions very inefficient, $r \approx 0$.

3.4. Flow Transition: Emergent to Unconfined

As the depth ratio increases from the emergent limit (H/h = 1), the canopy flow evolves through a continuum of conditions. The most fundamental shift is that of the mean momentum budget. Flow in an emergent canopy (Figure 1c) is determined by the gradient of pressure and/or elevation head and vegetative drag. As forcing is uniformly distributed in the vertical, the velocity profile is determined by the variation in vegetative drag. As the depth ratio increases, a shear layer develops at the top of the canopy (e.g., Figure 1b), and turbulent stress imposed from above begins to contribute momentum to the flow within the canopy. The contribution of turbulent stress increases with depth ratio and dominates the in-canopy momentum for H/h >10. Beyond this depth ratio, canopy flow is determined solely by vertical turbulent exchange of momentum. This limit is documented in terrestrial canopies [e.g., *Kaimal and Finnigan*, 1994].

Once a canopy becomes submerged, the vertical penetration of turbulent stress defines a vertical exchange zone. The depth of this region increases with the depth ratio. This trend is depicted in Figure 9a for the canopy studied here and for other canopies reported in the literature. For a given canopy density the penetration depth, h_p, asymptotes to an unconfined limit at $H/h \approx 2$. The penetration depth is determined in part by the scale of the active turbulence at the top of the canopy, $L_S \sim h$ [*Raupach et al.*, 1996], which is diminished for $H/h < 2$, but becomes constant for $H/h > 2$ (Figure 9b). This suggests that for $H/h < 2$ the penetration depth is reduced because L_S is constrained by the water depth. When L_S is unconstrained, the limiting penetration depth is determined by the canopy density, a, with greater penetration observed for sparser canopies, *i.e.* for canopies that provide less momentum absorption (Figure 9a). For $H/h > 2$, eddies larger than h are also present above the canopy, but these scales contribute little to turbulence within the canopy [*Raupach et al.*, 1996]. It is useful to note that the zero-plane displacement, d, follows h_p, with $d \approx h_p/2$ (Figure 9b), and thus may be a useful estimator for the extent of the vertical exchange zone.

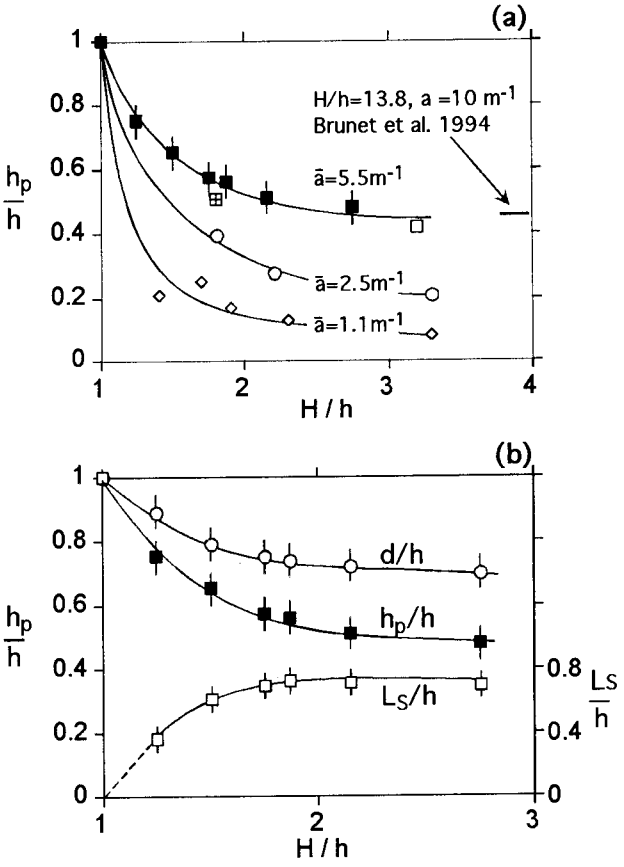

Figure 9. Transition from emergent (H/h =1) to unconfined submerged conditions. a) Penetration depth, h_p, based on Reynolds stress: present study (solid squares); *Dunn et al.* [1996] (diamonds and open circles); *Murato et al.* [1984] (square with cross); and *Seginer et al.* [1976] (open square). (b) Comparison of penetration depth (solid squares) and zero-displacement height, d (open circles). The shear length scale, L_S (open squares), is plotted on the right-hand axis.

The shift in penetration depth can describe the evolution of exchange dynamics from emergent to unconfined conditions. For emergent canopies, exchange with surrounding water occurs only through longitudinal advection. In addition, the canopy turbulence is largely wake generated, and its small scale makes diffusive transport within the canopy slow. As the depth ratio increases, the upper canopy communicates with the overlying water through vertical turbulent exchange. Much of the turbulence in this region is shear generated. Because the shear turbulence is of significantly larger scale than the wake turbulence, it quickly dominates transport and elevates turbulent diffusion in the canopy.

4. Summary and Extension to Other Canopies

Laboratory experiments on a scaled model reveal two distinct flow zones within an aquatic canopy. The lower canopy, called the "longitudinal exchange zone," exchanges with surrounding water predominantly through longitudinal advection. In this region, turbulence is generated within stem wakes and scales on the stem morphology. Turbulence levels are strongly dependent on the stem Reynolds number, which dictates the stem wake conditions. The momentum

budget is a simple balance of vegetative drag and hydrodynamic pressure gradient (and/or bed slope), such that the mean velocity profile is set by the vertical structure of the vegetative drag. Thus both the mean and turbulent velocity is linked to the details of canopy morphology.

The upper canopy, called the "vertical exchange zone", exchanges with surrounding water predominantly through vertical exchange. In this region the mean and turbulent velocity characteristics are strongly influenced by the shear layer that forms at the top of the canopy. In contrast to the lower region, specific details of canopy morphology are of lesser importance to turbulent and mean velocity, only that the canopy produces sufficient drag to generate a shear layer.

The extent of each zone is set by the depth of submergence and by the canopy morphology, density, and flexibility. For emergent canopies, $H/h = 1$, only the longitudinal exchange zone is present. When the canopy becomes submerged, a vertical exchange zone appears at the top of the canopy and progressively deepens into the canopy as the depth of submergence increases from 1 to 2. Beyond this submergence h_P is set by the distribution of momentum absorption within the canopy, which depends on C_D and a. For example, canopies with higher canopy density, a, have shallower vertical exchange zones, as shown in Figure 9. Recall that a increases both with stem density, n, and with individual stem morphology, that is, frontal area, A_f (see (1)). Stem morphology and flexibility can further impact penetration depth through C_D. For example, a branched or dendritic stem will produce more drag per unit of frontal area, that is, higher C_D, than a smooth, cylindrical stem. In addition, when stems are flexible both a and C_D can be functions of velocity. With increasing flow speed, flexible plants progress from an erect posture (considered here) through increasing degrees of pronation and waving. Bending of the canopy increases the local frontal area, effectively increasing a at the top of the canopy. This trend suggests that h_P will decrease as canopy pronation increases. Extreme pronation will eliminate vertical exchange entirely by creating by a solid leaf barrier at the top of the canopy. In some flexible canopies, moderate, unidirectional flows produce coherent waving called "monami" [*Ackerman and Okubo*, 1993]. Preliminary laboratory studies suggest that vertical exchange is enhanced during monami events [*Ghisalberti*, 2000].

Acknowledgments. This work was completed under NSF CAREER Award, EAR 9629259. The authors thank Paul Fricker and Hrund Andradottir for providing useful comments. The second author was supported by a GEM Fellowship (1996-1997) and a NSF Graduate Fellowship (1997-1998).

References

Ackerman, J., and A. Okubo, Reduced mixing in a marine macrophyte canopy, *Funct.Ecol.*, *7*, 305-309, 1993.

Brunet, Y., J. Finnigan, and M. Raupach, A wind tunnel study of air-flow in waving wheat: Single-point velocity statistics, *Boundary Layer Meteorol.*, *70*, 95-132, 1994.

Burke, R., and K. Stolzenbach, Free surface flow through salt marsh grass, *MIT-Sea Grant Tech. Rep.*, *MITSG 83-16*, Mass. Inst. Technol., Cambridge, 1983.

Duarte, C. M., Seagrass depth limits, *Aquat. Bot.*, *40*, 363-377, 1991.

Dunn, C., F. Lopez, and M. Garcia, Mean flow and turbulence in a laboratory channel with simulated vegetation, *Rep. 51*, Hydraulic Eng. Ser., Univ. of Ill., Urbana, 1996.

Finnigan, J., Turbulence in waving wheat. I. Mean statistics and honami. *Boundary Layer Meteorol.*, *16*, 181-211, 1979.

Gambi, M., A. Nowell, and P. Jumars, Flume observations on flow dynamics in *Zostera marina* (eelgrass) beds, *Mar. Ecol. Prog. Ser.*, *61*, 159-169, 1990.

Ghisalberti, M., Mixing layer and coherent structures in vegetated aquatic flows, M.S. thesis. Mass. Inst. of Technol., Cambridge, 2000.

Grizzle, R., F. Short, C. Newell, H. Hoven, and L. Kindblom, Hydrodynamically induced synchronous waving of seagrasses: "Monami" and its possible effects on larval mussel settlement, *J. Exp. Mar. Biol. Ecol.*, *206*(1-2), 165-177, 1996.

Kadlec, R., Overland flow in wetlands: Vegetation resistance. *J. Hydraul. Eng.*, *116*, 691-707, 1990.

Kadlec, R., Overview: Surface flow constructed wetlands. *Water Sci. Technol.*, *32*, 1-12, 1995.

Kaimal, J., and J. Finnigan. *Atmospheric Boundary Layer Flows*, Oxford Univ. Press. New York, 1994.

Kouwen, N., and R. Li, Biomechanics of vegetative channel linings. *J. Hydraul. Div. Am. Soc. Civ. Eng.*, *106*(HY6), 1085-1103, 1980.

Kouwen, N., and T. Unny, Flexible roughness in open channels, *J. Hydraul. Div., Am. Soc. Civ. Eng.*, *99*(HY5), 713-727, 1973.

Kundu, P.K., *Fluid Mechanics*, 638 pp., Academic, San Diego, Calif., 1990.

Leonard, L., and M. Luther. Flow hydrodynamics in tidal marsh canopies, *Limnol. Oceanogr.*, *40*, 1474-1484, 1995.

Lopéz, F., and M. García, Open-channel flow through simulated vegetation: Suspended sediment transport modeling. *Water Resour. Res.*, *34*(9), 2341-2352, 1998.

Lumley, J., Interpretation of time spectra measured in high-intensity shear flows, *Phys. Fluids*, *8*(6), 1056-1062, 1965.

Munson, B., D. Young, and T. Okiishi, *Fundamentals of Fluid Mechanics*, John Wiley, New York, 1990.

Murato, A., T. Fukuhara, and M. Sato, Turbulence structure in vegetated open channel flows, *J. Hydrol. Hydraul. Eng.*, *2*(1), 47-61, 1984.

Nepf, H. M., Drag, turbulence and diffusion in flow through emergent vegetation. *Water Resour. Res.*, *35*(2), 479-489, 1999.

Nezu, I., and W. Rodi, Open-channel flow measurements with a laser Doppler anemometer. *J. Hydraul. Eng.*, *112*, 335-355, 1986.

Orth, R.J., and K.A. Moore, Distribution of *Zostera marina* and *Ruppia maritima sensu lato* along depth gradients in the lower Chesapeake Bay, USA, *Aquat. Bot.*, *32*, 291-305, 1988.

Raupach, M., and R. Shaw, Averaging procedures for flow within vegetation canopies, *Boundary Layer Meteorol.*, *22*, 79-90, 1982.

Raupach, M., R. Antonia, and S. Rajagopalan, Rough-wall turbulent boundary layers, *Appl. Mech. Rev.*, *44*(1), 1-25, 1991.

Raupach, M., J. Finnigan, and Y. Brunet, Coherent eddies and turbulence in vegetation canopies: The mixing-layer analogy. *Boundary Layer Meteorol.*, *60*, 375-395, 1996.

Seginer, I., P. Mulhearn, E. Bradley, and J. Finnigan, Turbulent flow in a model plant canopy, *Boundary Layer Meteorol.*, *10*, 423-453, 1976.

Shaw, R., Secondary wind speed maxima inside plant canopies, *J. Appl. Meteorol.*, *16*, 514-521, 1977.

Shi, Z., J. Pethick, and K. Pye, Flow structure in and above the various heights of a saltmarsh canopy: A laboratory flume study, *J. Coastal Res.*, *11*, 1204-1209, 1995.

Thom, A. S., Momentum absorption by vegetation, *Q. J. R. Meteorol. Soc.*, *97*, 414-428, 1971.

H. Nepf and E. Vivoni, Parsons Laboratory, Department of Civil and Environmental Engineering, Massachusetts Institute of Technology, Cambridge, MA 02139. (hmnepf@mit.edu)

(Received August 31, 1999; revised June 16, 2000; accepted August 9, 2000.)